Proposal of Sensorless Vehicle Detection Method for Start-up Current Control in Dynamic Wireless Power Transfer System

Takumi Hamada, Daisuke Shirasaki, Toshiyuki Fujita, Hiroshi Fujimoto
Department of Advanced Energy
The University of Tokyo
5-1-5, Kashiwanoha, Kashiwa, Chiba, 277-8561 Japan
Email:hamada.takumi21@ae.k.u-tokyo.ac.jp

***Abstract*—This paper discusses the start-up process for a dynamic wireless power transfer system to an electric vehicle passing a road-side coil. To transfer maximum energy in a short time, the process of detecting an approaching vehicle and transmitting power must be carried out quickly. In most of the previous studies, problems of vehicle detection and power transmission have been considered separately. In this paper, the power transmission control process is proposed that combines vehicle detection and current control. The detection process uses only vehicle-side voltage pulse which enables both road-side and vehicle-side coils to sense approaching of the vehicle-side coil. And the current control suppresses the current overshoot at the start of power transmission. The proposed method was verified by experiments. Both coils could detect another one at a sufficient distance from each other. Additionally, power transmission starts at a point of small coupling coefficient was achieved without current overshoot.**

***Index Terms*—wireless power transfer, dynamic charging, vehicle detection, current control**

I. Introduction

In recent years, the use of electric vehicles (EVs) is expected to increase instead of internal combustion engine vehicles in the future, as a solution to environmental problems and the lack of fossil fuels. However, EVs have some problems such as a shorter cruising range per charge and longer charging time compared to conventional vehicles. Therefore, a dynamic wireless power transfer (DWPT) system, which applies a wireless power transfer (WPT) system technology to EVs, has been studied as a drastic solution to this problem [1].

WPT has been widely studied in the past [2]–[4]. In particular, WPT using magnetic resonance coupling enables high-efficiency and high-power transmission even with a large air gap between a transmitting coil and a receiving coil [5]–[7]. DWPT is expected to solve the above problems, such as cruising distance, charging time, and reducing battery installed in EVs, which will lead to cost reduction.

The process of DWPT can be divided into three stages: vehicle detection, transient response, and steady-state power supply. In general, DWPT systems with a very long road-side coil are expected to lose efficiency due to the large magnetized road area, which causes high conduction losses. Thus, the authors assume a system with a large number of short coils of less than 1.5 m on the roadside [8]. In this case, the process such as vehicle detection and transient response will occupy a large proportion of the system and are important. The system needs to transmit power within a limited time and the time becomes shorter as higher the speed of a vehicle increase. For example, if the vehicle is traveling at a speed of 80 km/h on the highway and the size of a road-side coil is 1 m, the time of the power transfer is only 45 ms at a road coil. Therefore, it is important to reduce the time required for vehicle detection and transient response and to maintain the power supply time as much as possible.

In the previous studies on DWPT, some groups proposed a vehicle detection method using the road-side current for sensor-less detection [9], [10]. Also, another proposed method use detection coils and vehicle-side pulses for detection including lateral deviation [11]. Studies focus on transient response include those that propose models at the start of power transmission [12], methods using soft start current [13] and those that focus on power supply during coil passage [14].

As far, these studies have been considered independently, but it is important to integrate them to implement a DWPT system in the market. Thus, this paper proposes the power transmission control process that combines vehicle detection and current control in the case of passing a road-side coil.

First, section Ⅱ explains the previous study that the start-up current control method [15] and the sensorless vehicle detection method [16]. Next, and the method proposed to improve the detection method by utilizing the vehicle-side current to address the problems that occur when considering the combined method in the last section Ⅱ. In section Ⅲ and Ⅳ, the experimental setup and the results of the experiments using the proposed method are demonstrated respectively. Finally, conclusions and future work are presented.

II. Control method and simulation

As shown for circuit configuration in Fig. 1, a series-series (SS) compensated resonant topology with full-bridge converters on both sides is assumed. The circuit model assumes the vehicle side as a rectifier with a constant voltage load, which is suitable for EV use. The circuit parameters are shown in

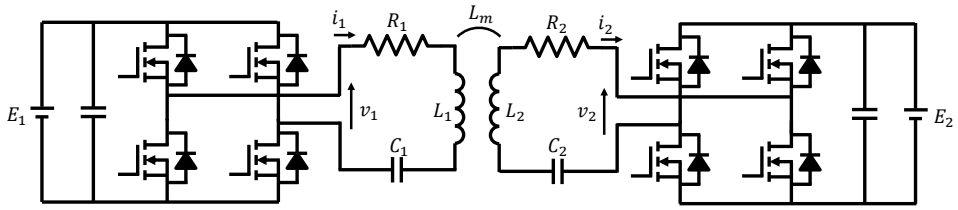

Fig. 1. SS-compensated circuit configuration for DWPT.

TABLE I
PARAMETERS IN THE SIMULATION AND THE EXPERIMENT.

Parameter	Value
Operating frequency f_o	84.5 kHz
Road-side inductance L_1	250.9 μH
Road-side resistance R_1	279.3 mΩ
Vehicle-side inductance L_2	96.5 μH
Vehicle-side resistance R_2	186.9 mΩ
Road-side DC-link voltage E_1	10 V
Vehicle-side DC-link voltage E_2	10 V

Table I. Converters are driven by phase-shift control and output an AC voltage with the following amplitude of a fundamental component.

$$V_{ac} = \frac{4}{\pi} E_{dc} \sin\left(\frac{\pi}{2} d\right) \tag{1}$$

Here DC voltage E_{dc} and duty ratio d.

Mainly, the converter on the road-side is used for current control, and the converter on the vehicle-side is used for the vehicle detection method. Details are given in the respective sections.

A. Start-up current control

The study [15] uses the start-up current control using the envelope model. In this method, the envelope values are focused on the WPT circuit by modeling using phaser coordinate, not assuming the instantaneous values. This model decides two modes which are conducting the rectifier diodes or not conducting. Thereby, the method allows for accurate envelope modeling.

The modeling equation is expressed as a nonlinear state equation with state variables and input variables as follows.

$$\dot{\boldsymbol{x}}(t) = \boldsymbol{f}\left(\boldsymbol{x}(t), \boldsymbol{u}(t)\right) \tag{2}$$

$$\boldsymbol{y}(t) = \boldsymbol{g}\left(\boldsymbol{x}(t)\right) = \sqrt{i_{1d}^2 + i_{1q}^2} \tag{3}$$

$$\boldsymbol{x} = [i_{1d}, i_{1q}, i_{2d}, i_{2q}, v_{C1d}, v_{C1q}, v_{C2d}, v_{C2q}]^{\mathrm{T}} \tag{4}$$

$$\boldsymbol{u} = v_{1d} = |v_1| \tag{5}$$

Here road-side current i_1, vehicle-side current i_2, road-side capacitor voltage v_{C1}, vehicle-side capacitor voltage v_{C2}, road-side voltage v_1, and vehicle-side voltage v_2. The subscripts indicate the d-axis and q-axis, respectively. Further discussions are done in [15].

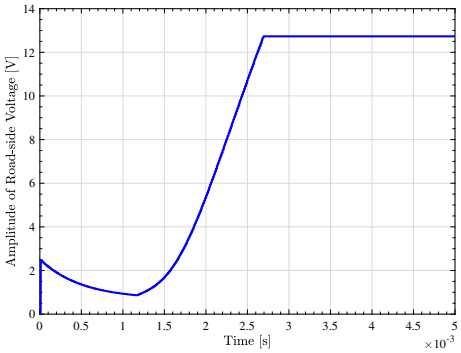

Fig. 2. The amplitude of road-side voltage calculated by an offline high-gain feedback calculation.

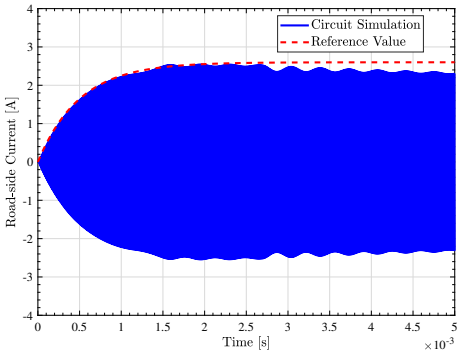

Fig. 3. Simulation result with start-up current control.

Based on the envelope model, the trajectory of the amplitude of road-side voltage $\boldsymbol{u}(t)$ should be derived that the envelope of road-side current $\boldsymbol{y}(t)$ is the reference trajectory $\boldsymbol{y_{ref}}(t)$. However, while the envelope model is very accurate, it is difficult to calculate it analytically because of its nonlinearity, where the state equation and output equation change significantly with conduction and non-conduction. Therefore, the desired trajectory $\boldsymbol{u}(t)$ is calculated by an offline high-gain feedback calculation [17].

Fig. 2 shows the input voltage trajectory that is calculated from the reference road-side current envelope trajectory. Fig. 3 shows the MATLAB simulation results when the input signal is using by Fig. 2. To eliminate the overshoot of input current which occurred at the charging starts, the reference waveform of the amplitude of road-side current i_1 in the control method was a first-order time delay response. The waveform rises slowly to follow the trajectory of the road-side

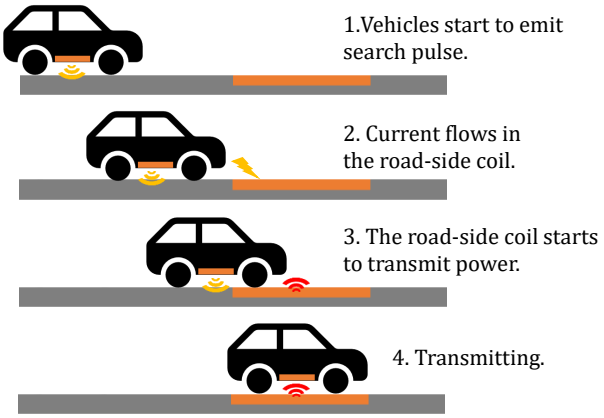

Fig. 4. The detection method in which search pulses are transmitted from the vehicle-side coil.

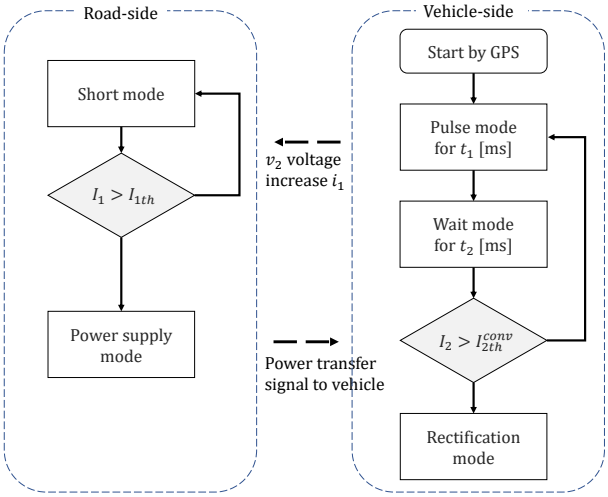

Fig. 5. State transition diagram of conventional method.

current envelope and suppress the overshoot of the current.

B. Conventional vehicle detection method

This section describes the sensorless vehicle detection method [16] that is the basis of the proposed method. This method proposes to emit detection voltage pulses from the vehicle-side to inform the road-side coil of the approaching vehicle. It has a high sensitivity of detection with no additional sensors or coils.

The diagram of the method is shown in Fig. 4. First, the vehicle acquires information that it is approaching the wireless power supply section through wireless communication such as GPS, and then the vehicle starts applying detection pulses. Next, when the vehicle approaches the road-side coil, an induced current flows on the road-side coil due to the coupling between both coils. When the amplitude of the road-side induced current exceeds a current threshold I_{1th}, the road-side inverter starts to transmit power. At the same time, the vehicle side converter switches from the search mode to the rectification mode when the amplitude value of the current transmitted from the road-side exceeds a certain threshold current I_{2th}, and then it starts to receive power.

Fig. 5 shows the state transition diagram of this method. Switching of converters realizes each mode. The short mode means turning on the lower switches of the vehicle-side converter and the AC voltage set to zero. The pulse mode emits detection pulses using the voltage pulses of a lower duty ratio than the power supply mode. The wait mode emits no voltage pulse, so it is the same as in the rectification mode. Also, the processes of the pulse mode and wait mode are collectively called the search mode.

In the road-side coil, the coil waits in the short mode to make it easier to detect the induced current. It also has the advantage of simplifying the current threshold design since the effect of the road-side DC voltage can be ignored. The threshold current I_{1th} for vehicle detection is a designed value depending on the coupling coefficient. In the vehicle-side coil, the system alternates between the pulse mode and the wait mode. The wait mode is inserted due to save power consumption and due to suppress the transient response.

The problem of this method occurs in the power transmission from the road-side unit to the vehicle-side. The vehicle-side coil cannot recognize the presence of the road-side coil until the power transmission starts and continues to emit the detection pulse. If the detection pulse and power transmission occur at the same time, a large current is generated.

C. Proposed detection method

To solve the above problem, the vehicle-side coil needs to notice the presence of the road-side coil before the power is transmitted. Therefore, the vehicle-side and road-side coils detect each other using only the vehicle-side pulses is proposed.

The proposed method focuses on the trend of induced current. When the vehicle-side is in the pulse mode, each amplitude of currents is expressed as follows [16].

$$I_1 = \frac{\omega_0 \sqrt{L_1 L_2} k}{R_1 R_2 + \omega_0^2 k^2 L_1 L_2} V_2 \tag{6}$$

$$I_2 = \frac{R_1}{R_1 R_2 + \omega_0^2 k^2 L_1 L_2} V_2 \tag{7}$$

Here resonance frequency ω_0, coupling coefficient k, and the amplitude of vehicle-side voltage V_2. Fig. 6 shows the relation between the induced currents using the parameters in Table I to the coupling coefficient when the duty ratio of the voltage pulse width is 0.05. The conventional method detects the road-side induced current based on its upward trend, but the vehicle-side induced current has a downward trend, so the vehicle-side coil can detect the road-side coil when the pulse current drops below the threshold. In the conventional method, the vehicle-side pulse current is used only for the threshold judgment of the road-side. Thus, it can be effectively used for the vehicle side as well by this process. By designing the current thresholds of coils appropriately, bilateral coil detection can be realized. Specifically, the vehicle-side current needs to exceed the threshold after the road-side one exceeds the threshold.

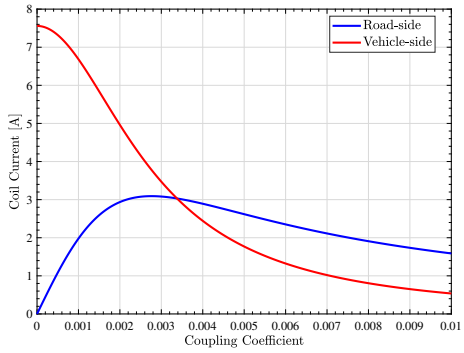

Fig. 6. Coil induced current as function of coupling coefficient (duty ratio $d = 0.05$).

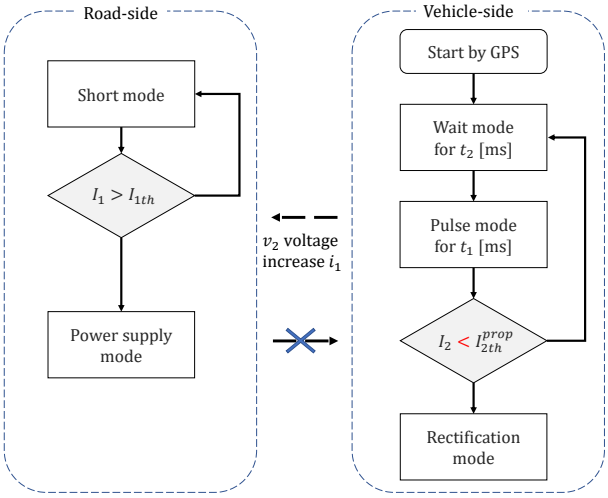

Fig. 7. State transition diagram of proposed method.

Fig. 7 shows the state transition diagram of this method. The major difference compared with Fig. 5 is that the detection method of the vehicle-side has been changed. In the conventional method, the vehicle-side starts receiving power by detecting the increase in current as the road-side starts transmitting power. Whereas, in the proposed method, the vehicle-side detection pulses alone can detect each other's coils.

III. Experimental setup

To demonstrate the effect of the proposed method, the DWPT bench as the experimental setup is used as shown in Fig. 8(a). Fig. 8(b) shows the vehicle-side coil and the road-side coil. The speed of the vehicle-side coil is 5 km/h. Fig. 8(c) is the inverters for the experiment at the both sides of the circuit diagram shown in Fig. 1, and the fundamental amplitude of the AC voltage is manipulated by driving three levels of a full-bridge converter. Fig. 9 shows the relation of the coupling coefficient from the center of the coil.

Fig. 10 shows a flow of the experiments. In the conventional method, a) and c) only are implemented. In the proposed method, a), b), and c) are implemented. The wait-time is designed by the position of the power transfer, the vehicle speed, and the detection point. The wait-time is set up because the vehicle detection method can detect the coils from the negative coupling region but the vehicle-side cannot receive power near the null point. The speed of the vehicle is assumed to be known in this experiment. It is not unreasonable to assume that the vehicle will be traveling at a certain speed when automatic driving becomes widespread in the future. These positions can be determined by the desired coupling coefficient and designing the current threshold. In this experiment, the positions of the points a), b), c) set to −650 mm, −580 mm, and −450 mm, respectively. Fig. 11 shows the position where each process occurs. Note that this method can detect the bilateral

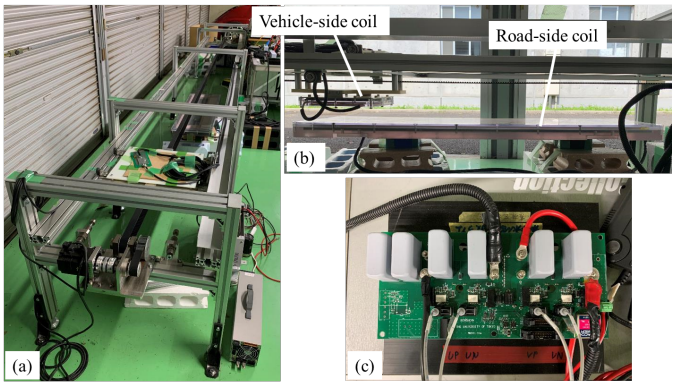

Fig. 8. Experimental setup (a) DWPT bench (b) coils (c) inverter.

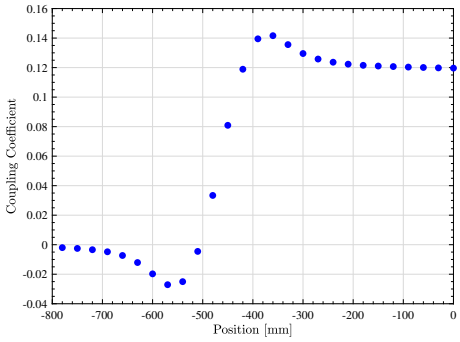

Fig. 9. Experimental results of the coupling coefficient and varying distance from the center of road-side coil.

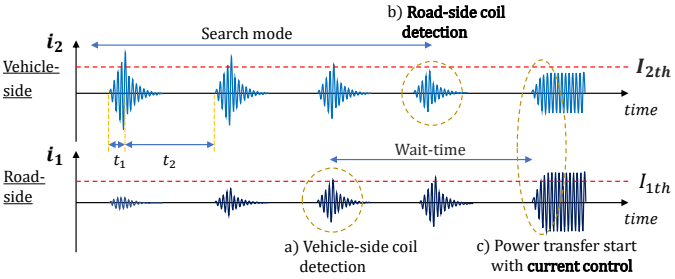

Fig. 10. Image of the experimental flow (conventional method : a) → c), proposed method : a) → b) → c)).

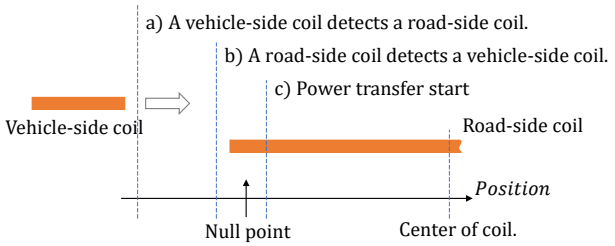

Fig. 11. Position of coils in each process.

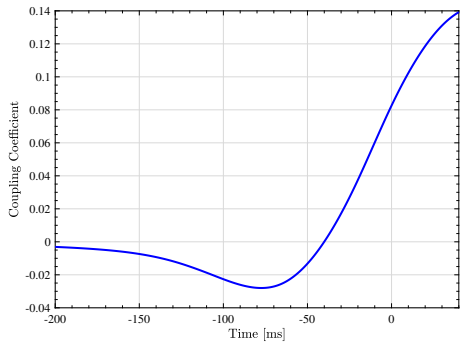

Fig. 12. Expected coupling coefficient in the experiment (the speed of the vehicle-side coil is 5 km/h).

coil in the negative coupling region. The amplitude of the AC voltage on the roadside, which is the control input quantity, is shown in Fig. 2. This time, the period of the two modes set $t_1 = 1$ ms and $t_2 = 3$ ms respectively as in the literature [16].

IV. Experimental results

A. Conventional detection method and current control

Figs. 12, 13 show the coupling coefficient and the experimental results of the combination of the conventional detection method and current control. This result is an example of overlap, where the detection pulse and the start of power transmission occur simultaneously.

Initially, the road-side is in the short mode and the vehicle-side is in the search mode. At about −140 ms, the road-side current exceeds I_{1th}, and after a wait-time, it changes to the power supply mode at 0 ms as shown in Fig. 13(b). At this time, the vehicle-side remains in the search mode because there is not enough current. After that, power transmission is performed from both the road-side and the vehicle-side. In this case, a large overshoot of the current occurs at 2.2 ms as shown in Fig. 13(c). Finally, the vehicle-side goes into the rectification mode, and although there is some vibration, power is transmitted normally.

The increase in the vehicle-side current around −40 ms is due to the change in the resonance frequency. The reason is the change in the self-inductance of the vehicle-side coil due to the effect of the ferrite in the road-side coil. If the self-inductance does not fluctuate, the current is expected to be similar to the current around −200 ms, when the coupling is weak.

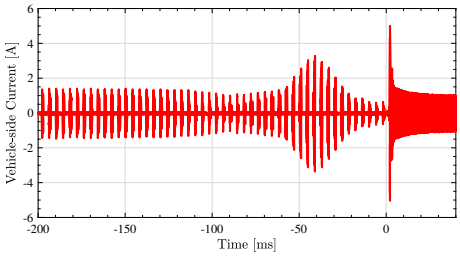

(a) Vehicle-side current.

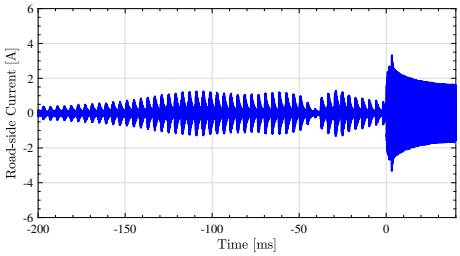

(b) Road-side current.

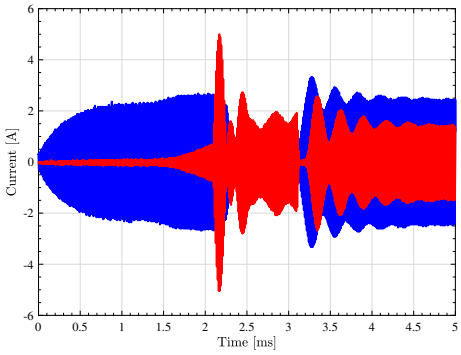

(c) Currents in the start of power transmission.

Fig. 13. Experimental results of conventional method in the case where the vehicle-side detection pulse and the start of power transmission overlap.

Cases where power transmission is started properly or where the pulse and power transmission timing match perfectly can also occur. In any case, this method cannot be applied to achieve a stable power transmission process.

B. Proposed detection method and current control

The experimental results of the combination of the proposed detection method and current control are shown in Fig. 14.

As in the conventional method, in the initial state, the road-side is in the short mode and the vehicle-side is in the search mode. The difference of the proposed method is that the mode of the vehicle-side changes from the search mode to the rectification mode before the power transmission starts. As shown in Fig. 14(a), the vehicle-side current drops below I_{2th} at about 100 ms, then the rectification mode is activated. As a result, the power transmission starts by the start-up current control, and the vehicle-side coil receives the power properly without overshoot as shown in Fig. 14(c). Also, the decrease in the current after 0 ms is due to the increase in the coupling coefficient, and the same phenomenon is observed in the conventional method.

The maximum detection deviation caused by the experiment was about 6 mm. Theoretically, when the detection cycle is 4 ms and the speed is 5 km/h, the misalignment is about 5.6 mm. Therefore, if the current threshold can be properly determined, the detected deviation is expected to be approximately dependent on the detection resolution and speed. In this experiment, even in the case of the maximum detection deviation the current control without current overshoot as shown in Fig. 14(c) was achieved.

V. Conclusion

In this paper, a combination of vehicle detection and start-up current control was conducted. To solve the problem that the detection pulse and the start of power transmission overlap, a novel detection method was proposed. In this method, the coils detect each other using only the vehicle-side detection pulse. The effect of the proposed method was verified by experiment. Both coils could detect another one at a sufficient distance from each other. And power transmission starts at a point of small coupling coefficient was achieved without current overshoot.

VI. Acknowledgement

This work was partly supported by JST-Mirai Program Grant Number JPMJMI21E2, JSPS KAKENHI Grant Number JP18H03768, Japan.

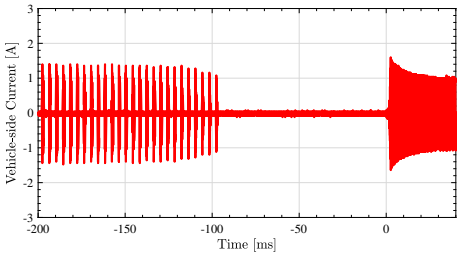

(a) Vehicle-side current.

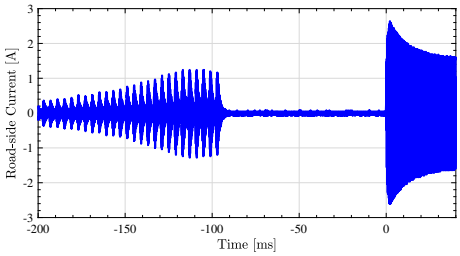

(b) Road-side current.

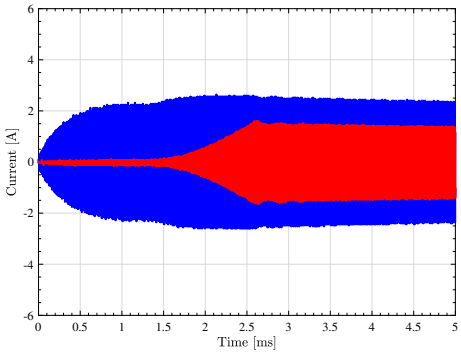

(c) Currents in the start of power transmission.

Fig. 14. Experimental results of proposed method.

References

[1] S. Li and C. C. Mi, "Wireless Power Transfer for Electric Vehicle Applications," *IEEE Journal of Emerging and Selected Topics in Power Electronics*, vol. 3, no. 1, pp. 4–17, 2015.

[2] Z. Zhang, H. Pang, A. Georgiadis, and C. Cecati, "Wireless Power Transfer - An Overview," pp. 1044–1058, 2019.

[3] H. Matsumoto, T. Zaitsu, R. Noborikawa, Y. Shibako, and Y. Neba, "Control for Maximizing Efficiency of Three-Phase Wireless Power Transfer Systems At Misalignments," *IEEJ Journal of Industry Applications*, vol. 9, no. 4, pp. 401–407, 2019.

[4] K. Kusaka, K. Furukawa, and I. Junichi, "Development of three-phase wireless power transfer system with reduced radiation noise," *IEEJ Journal of Industry Applications*, vol. 8, no. 4, pp. 600–607, 2019.

[5] A. Kurs, A. Karalis, R. Moffatt, J. D. Joannopoulos, P. Fisher, and M. Soljačić, "Wireless power transfer via strongly coupled magnetic resonances," *Science*, vol. 317, no. 5834, pp. 83–86, 2007.

[6] M. Fu, Z. Tang, and C. Ma, "Analysis and Optimized Design of Compensation Capacitors for a Megahertz WPT System Using Full-Bridge Rectifier," *IEEE Transactions on Industrial Informatics*, vol. 15, no. 1, pp. 95–104, 2019.

[7] J. Feng, Q. Li, F. C. Lee, and M. Fu, "LCCL-LC Resonant Converter and Its Soft Switching Realization for Omnidirectional Wireless Power Transfer Systems," *IEEE Transactions on Power Electronics*, vol. 36, no. 4, pp. 3828–3839, 2021.

[8] H. Fujimoto, O. Shimizu, S. Nagai, T. Fujita, D. Gunji, and Y. Ohmori, "Development of wireless in-wheel motors for dynamic charging: From 2nd to 3rd generation," *2020 IEEE PELS Workshop on Emerging Technologies: Wireless Power Transfer, WoW 2020*, pp. 56–61, 2020.

[9] A. Ong, P. K. S. Jayathurathnage, J. H. Cheong, and W. L. Goh, "Transmitter pulsation control for dynamic wireless power transfer systems," *IEEE Transactions on Transportation Electrification*, vol. 3, no. 2, pp. 418–426, 2017.

[10] D. Kobayashi, K. Hata, T. Imura, H. Fujimoto, and Y. Hori, "Sensorless vehicle detection using voltage pulses in dynamic wireless power transfer system," *EVS 2016 - 29th International Electric Vehicle Symposium*, pp. 1–10, 2016.

[11] A. N. Azad, A. Echols, V. A. Kulyukin, R. Zane, and Z. Pantic, "Analysis, optimization, and demonstration of a vehicular detection system intended for dynamic wireless charging applications," *IEEE Transactions on Transportation Electrification*, vol. 5, no. 1, pp. 147–161, 2019.

[12] Y. Guo, L. Wang, Q. Zhu, C. Liao, and F. Li, "Switch-On Modeling and Analysis of Dynamic Wireless Charging System Used for Electric Vehicles," *IEEE Transactions on Industrial Electronics*, vol. 63, no. 10, pp. 6568–6579, 2016.

[13] W. Zhong, H. Li, S. Y. Hui, and M. D. Xu, "Current Overshoot Suppression of Wireless Power Transfer Systems with on-off Keying Modulation," *IEEE Transactions on Power Electronics*, vol. 36, no. 3, pp. 2676–2684, 2021.

[14] G. Guidi and J. A. Suul, "Transient Control of Dynamic Inductive EV Charging and Impact on Energy Efficiency when Passing a Roadside Coil Section," *2018 IEEE PELS Workshop on Emerging Technologies: Wireless Power Transfer, Wow 2018*, 2018.

[15] K. Tokita, H. Fujimoto, and Y. Hori, "Feedforward transient control under varying coupling condition for in-motion wireless power transfer using envelope model," *2020 IEEE Wireless Power Transfer Conference, WPTC 2020*, pp. 166–169, 2020.

[16] D. Shirasaki, H. Fujimoto, and Y. Hori, "Sensorless vehicle detection using vehicle side voltage pulses for in-motion WPT," *2020 IEEE PELS Workshop on Emerging Technologies: Wireless Power Transfer, WoW 2020*, pp. 320–325, 2020.

[17] G. C. Goodwin, S. F. Graebe, and M. E. Salgado, *Control System Design*, 1st ed. USA: Prentice Hall PTR, 2000.